17th World Conference on Earthquake Engineering, 17WCEE
Sendai, Japan - September 13th to 18th 2020

Effects of Uncertainties in Shear-Wave Velocity on Nonlinear Seismic Site Response Analysis Validated using Downhole Array Recordings

R. Boushehri[(1)], K. Ellison[(2)], K. Stanton[(3)], R. Motamed[(4)]

[(1)] *Graduate Research Assistant, University of Nevada, Reno, Rboushehri@nevada.unr.edu*
[(2)] *Associate, Arup, San Francisco, Kirk.Ellison@arup.com*
[(3)] *Analyst, Arup, San Francisco, kevin.stanton@arup.com*
[(4)]*Associate Professor, University of Nevada, Reno, motamed@unr.edu*

Abstract

This study quantifies the effects of uncertainties associated with the small-strain Vs profiles on nonlinear site response analysis results. A well-instrumented geotechnical downhole array site located in Japan is selected as our case study. Taxonomy screening was previously carried out to assess the extent of site complexity demonstrating the suitability of this site for one-dimensional site response analysis. A one-dimensional model of the site is developed in the finite element program LS-DYNA and the dynamic stress-strain relationship is characterized with a nonlinear backbone curve formulation capable of capturing the soil behavior at large shear strains. Uncertainties in dynamic soil properties are quantified using the Coefficient of Variation (COV) based on observed variability in measured in-situ shear wave velocity profiles. Measured and predicted site response, using recorded ground motions at this geotechnical downhole array, are compared to assess the significance of this uncertainty on the observed biases. The results show that the standard deviation of the responses is much greater at short periods than long periods, and the transition point can be estimated as one-fourth of the site period.

Keywords: Probabilistic seismic hazard assessment; Soil dynamics; Site response; Earthquake ground motions.

1. Background and Introduction

In recent years, several studies have highlighted the importance of downhole arrays to verify the accuracy of site response analysis [1-4]. Although these densely-instrumented arrays are usually well-documented, numerical modeling of these arrays still show some deviation from the recordings. There are several sources of uncertainty such as Vs profile [5-9], nonlinear dynamic soil properties [10-12], input motion selection [13-15] and analysis method [16-19], which may be responsible for deviations of predictions (deterministic approaches), from the actual site responses (recordings). Therefore, probabilistic seismic hazard analysis (PSHA), as complementary to deterministic analysis methods, can be of great importance, especially when safety-critical structures such as nuclear facilities, skyscrapers, etc. are involved [20, 21].

Several past studies have aimed to quantify the uncertainty of the small-strain Vs profile and/or Vs_{30} measurements [24-28]. This uncertainty is often considered in engineering practice by taking upper-and lower-bound Vs profiles. These upper/lower-bound profiles are usually generated by arbitrarily increasing and decreasing the reference Vs profile by a constant factor. This approach is first presented by the Electric Power Research Institute (EPRI) [35]. Based on the EPRI guideline, a minimum depth-independent standard deviation value (σ_{ln} (Vs)) of 0.25 should be considered for sites similar to the SHA. However, other studies have shown that the EPRI approach sometimes under/over estimates the site response [28]. In addition, the Vs profiles resulting from the EPRI method often do not agree with site-specific measurements. Toro 1995 [24] computed σ_{ln} (Vs) based on the time-weighted shear-wave velocity of the top 30m (Vs_{30}), using 541 profiles for the Vs_{30} USGS classification. The values for σ_{ln} (Vs) for different average shear-wave velocities are shown in Table 1.

Table 1 – Standard deviations computed by Toro (1995)

Vs_{30} (m/s)			
>750	360 to 750	180 to 360	<180
0.36	0.27	0.31	0.37

The purpose of the present study is to quantify the effect of uncertainties associated with the small-strain Vs profiles and backbone curves up to the target shear strength on nonlinear (NL) site response analyses. To this end, recordings from a very well-instrumented vertical downhole array (the Service Hall Array) are utilized as an example case study. The SHA contains four three-component accelerometers at depths of 2.4m (Holocene dune sand), 50.8m (Pliocene Banjin formation), 99.4m (Pliocene Nishiyama formation), and 250m (Pliocene Nishiyama formation) [3, 31]. Vs_{30} for the SHA is 199.3m/s based on P-S suspension logging. Fig. 1 shows the location of the Service Hall Array (SHA) near the Kashiwazaki-Kariwa Nuclear Power Plant (KKNPP) in Japan. Taxonomy screening was previously carried out at this site to assess the extent of site complexity which demonstrated its suitability for one-dimensional bi-directional site response analysis [2, 22, 23]. Liquefaction and basin effects are not considered to be significant at the SHA.

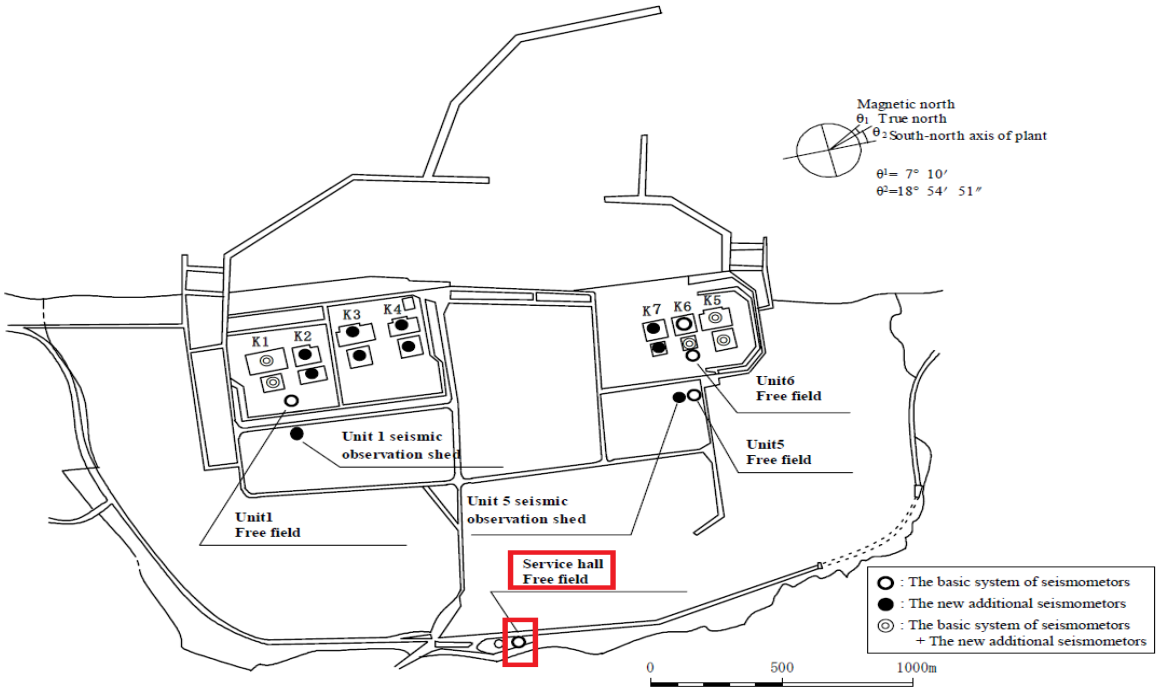

Fig. 1. Location map of the seismic observation point in the KKNPP (image provided by the Tokyo Electric Power Company).

2. Methodology

The ground motion recording selected for this study is from the 2007 Mw = 6.6 Niigata-Ken Chetsu-Oki earthquake, which occurred off the coast of Niigata. The essentially unprocessed data provided by the Tokyo Electric Power Company (TEPCO) is filtered in the same manner as described by Stewart et al. (2012) [32]. The processed acceleration time histories are then rotated in the fault normal and fault parallel directions and applied simultaneously in a bi-directional manner to the base of a site response model in the finite element software LS-DYNA [1]. The reference Vs profile utilized in this study is based on the P-S suspension logging data described by Yee et al. (2013) [3]. The base SRA model consists of 52 layers with the maximum shear modulus (G_{max}) for each layer corresponding to the shear wave velocity and mass density for the middle of the layer (Eq. (1)).

$$G_{max} = \rho V_s^2 \tag{1}$$

A modified two-stage hyperbolic backbone curve is then implemented for each layer to accurately model the nonlinear behavior of the soil materials. For this purpose, the LS-DYNA software is compiled with the MATLAB programming language and the desired NL constitutive models are incorporated into the program. Eq. (2) is implemented for the first stage of the hyperbolic backbone curve (hyperbola 1).

$$\tau = \frac{G_{max}\,\gamma}{1+\beta\left(\frac{\gamma}{\gamma_r}\right)^{\alpha}} \qquad \text{For } \gamma < \gamma_1 \tag{2}$$

where, γ is shear strain; γ_r represents pseudoreference strain; and α and β are fitting parameters. The above-mentioned equation can also be presented as follows.

$$\frac{G}{G_{max}} = \frac{1}{1+\beta(\frac{\gamma}{\gamma_r})^{\alpha}} \qquad \text{For } \gamma < \gamma_1 \tag{3}$$

The pseudoreference strain (γ_r) and the coefficient α can also be separately calculated using Eq. (4) and Eq. (5).

$$\alpha = \alpha_1 + \alpha_2 log(\frac{\sigma_0'}{P_a}) \tag{4}$$

$$\gamma_r = \gamma_{r,1}(\frac{\sigma_0'}{P_a})^n \tag{5}$$

where, σ_0' is the effective stress in the middle of each layer; and P_a is the atmospheric pressure. The values for α_1 , α_2, n, and $\gamma_{r,1}$ are estimated based on resonant column-torsional shear (RCTS) tests. For depths shallower than the water table (down to 45.5m), the values for α_1 and α_2 are assumed to be 0.82 +/- 0.1 and 0.34 +/- 0.27, respectively, based on the RCTS tests conducted by Stewart and Yee (2012) [33]. Beyond the water table depth, as test data is not available and matric suction is zero, constant values of 0.86 and 0.1 are recommended by Menq (2003) [34] for α_1 and α_2, respectively [34]. The estimated values for $\gamma_{r,1}$ and n to a depth of 20m, where the deepest sample was taken by Stewart and Yee (2012) [33], are 0.0904 and 0.4345, respectively. Similarly, for depths beyond this point, constant values of 0.0684 and 0.4345, suggested by Menq (2003) [34] are employed in the model.

Equation 6 represents the second portion of the hyperbolic backbone curve (hyperbola 2).

$$\frac{G}{G_{max}} = \frac{\frac{\gamma_1}{1+\beta(\frac{\gamma_1}{\gamma_r})^{\alpha}} + \frac{(\frac{G_{\gamma_1}}{G_{max}})\gamma'}{1+\beta'(\frac{\gamma'}{\gamma'_{ref}})}}{1+\beta(\frac{\gamma}{\gamma_r})^{\alpha'}} \qquad \text{For } \gamma > \gamma_1 \tag{6}$$

where, γ_1 is the user defined transition strain; G_{γ_1} is the tangent shear modulus corresponding to the transition strain and its corresponding stress (τ_1); β' and α' are curve-fitting parameters; γ'_{ref} represents the strength based reference strain; and $\gamma' = \gamma_1 - \gamma$.

$$\gamma'_{ref} = (\frac{\tau^*_{ff} - \tau_1}{G_{\gamma_1}}) \tag{7}$$

$$\tau^*_{ff} = a\,\tau_{ff} \tag{8}$$

where, τ^*_{ff} is pseudo-failure shear stress; and a is the shear strength coefficient. The procedure of choosing different values for the above-mentioned parameters and developing the second portion of the hyperbolic backbone curve is the same as described by Motamed et al. 2016 [1].

As mentioned earlier, the purpose of this study is to propose a procedure to separately calculate the contribution of uncertainty associated with small-strain shear-wave velocity to the total uncertainty in the NL

site response analysis results. Therefore, the shear strength is assumed to be constant for all models. This assumption may encourage failure/localization at small strains. The curve-fitting procedure for all of the randomizations is performed in a way that prevents localization from happening before the transition strain. In this study, as mentioned earlier, the Vs profile obtained from the P-S suspension logging test is considered as the reference small-strain Vs profile (as it is the only Vs profile available for SHA) and the randomization is performed using this profile.

Three levels of uncertainty associated with the small-strain Vs profile are considered herein based on the literature and design codes available [24-28]. The Latin Hypercube Sampling (LHS) technique is used to generate a statistically significant number of samples of the model (100) for each level of uncertainty. This method is one of the most efficient methods of sampling in which marginal probability distributions for each variable simulated is preserved, while matching target correlations between variables. To do this, the LHS technique constructs a highly dependent joint probability density function for random variables, which allows good accuracy in the response parameters using only a small number of samples as compared with traditional sampling techniques in which a much larger number of realizations would be needed to converge to the desired confidence level [29, 30].

Stochastic processes are generated using different distribution models and also considering the significant effects of Coefficient of Variation (COV) on the results. Based on references such as Toro [24], three different uncertainty values (σ_{ln}(Vs) = 0.15, 0.25, and 0.35) were selected for the present study to produce a reasonable range of Vs profiles. The randomized Vs profiles considered in this study are shown in Fig. 2.

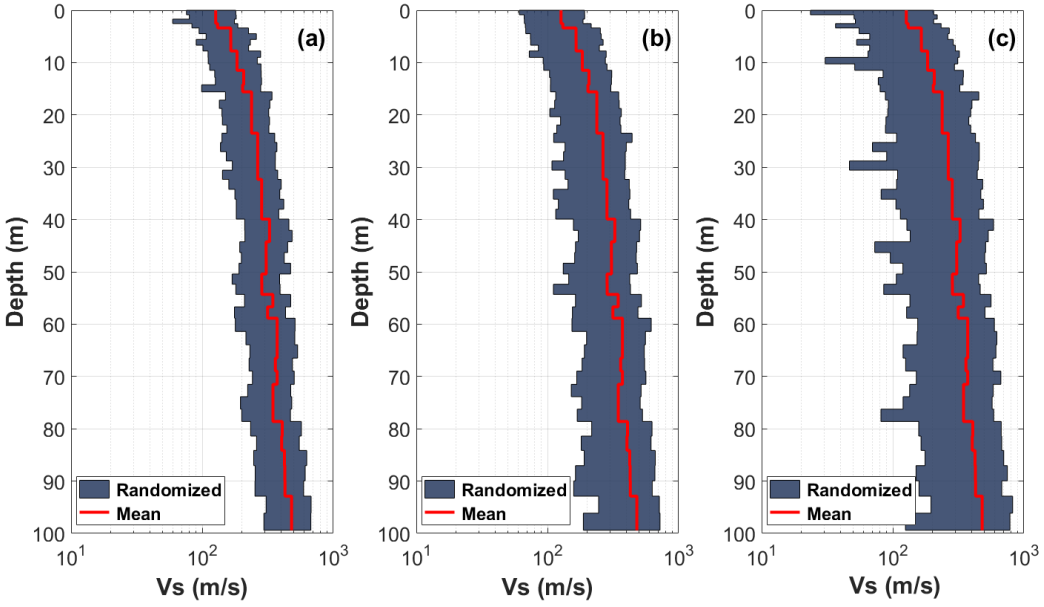

Fig. 2. Vs profiles developed to account for uncertainty at the Service Hall array. The Vs profile uncertainty is considered by randomizing the P-S suspension log Vs profile. Randomization performed using Latin Hypercube Sampling technique, and a total of 100 realizations are generated for each level of uncertainty. (a) σ_{ln}(Vs) = 0.15 (b) σ_{ln}(Vs) = 0.25, and (c) σ_{ln}(Vs) = 0.35).

3. Results

In this section, response spectra from recordings at the SHA are compared with predicted responses from the base model and various models with randomized Vs profiles.

Fig. 3 and Fig. 4 show the response spectra for depths of 2.4m and 50.8m, respectively (both in fault normal (FN) and fault parallel (FP) directions), considering a standard deviation value of $\sigma_{\ln}$ (Vs) = 0.25. As can be seen in both Fig. 3 and Fig. 4, there is more variability in the responses (i.e. greater standard deviations of amplification factors) at short periods than long periods. In addition, significant variability extends to higher periods in the FN direction due to greater amplitude shaking that results in more nonlinearity of the soil. This transition from significant to insignificant variability of the responses can be correlated to the predominant period range of the randomized Vs profiles. The predominant site period of the base model ($T_{Site,\ Vs}$), indicated in the figures, can be calculated using Eq. (9).

$$T_{Site,Vs} = 4\sum_{i=1}^{n}\frac{h_i}{V_{s_i}} \tag{9}$$

On the other hand, Eq. (10) represents the maximum wavelength that can affect each element of the soil profile.

$$\lambda_{\max} = h_i = V_{s_i}.T_i \tag{10}$$

Therefore, the approximate period corresponding to the maximum wavelength which may affect the whole soil profile (over a depth of 99.4 m), based on the average shear-wave velocity of the base model can be calculated (0.35 s). This period is referred to as the reference period (T_{ref}) in this study. This reference period can be correlated to predominant site period ($T_{Site,Vs}$) of the randomized Vs profiles. In other words, the term reference period (T_{ref}), presented in this study, provides an approximation of one-fourth of predominant site period ($T_{Site,Vs}$) of the randomized Vs profiles. Both (T_{ref}) of the base model and ($T_{Site,Vs}$)/4 of the randomized Vs profiles (shaded region) are indicated in the figures. As can be seen in Fig. 3, the standard deviation of the responses is greater for periods shorter than ($T_{Site,Vs}$)/4 of the randomized Vs profiles in comparison with the longer periods. Therefore, the cyan shaded area (one-fourth of predominant site period ($T_{Site,Vs}$) of the randomized Vs profiles), presented in the following graphs, can be referred to as the transition period, as the transition from significant to insignificant within the standard deviation of responses can be observed.

The variability of the response can also be attributed to the backbone curves generated for each layer. As discussed in the previous section, by changing the small-strain shear-wave velocity in each layer, the subsequent points of the backbone curves, up to the target shear stress, are also modified for each realization, which is responsible for this variability within the results for long periods (periods greater than the ($T_{Site,Vs}$)/4 of the randomized Vs profiles). It also can be concluded that the ratio of the bias associated with the small-strain Vs profile to the total bias of the system (measured based on the recordings) is greater in the FN direction compared to the FP direction, which is due to the different levels of strains in FN and FP directions. The strain profiles in both FN and FP directions are shown in Fig. 5.

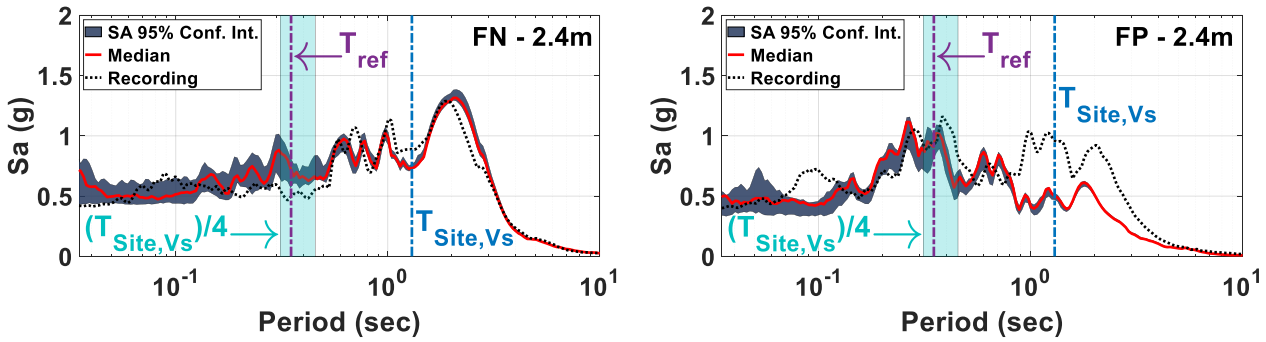

Fig. 3. 2D FN and FP response spectra for the depth of 2.4m below the ground surface (the depth of accelerometer 1). The data shown includes: predicted response spectra using all of 100 Vs profiles developed considering standard deviation value (σ_{ln} (Vs)) of 0.25 (blue area), recorded at accelerometer 1 (dotted black line), predicted response spectra of the base model with the reference Vs profile obtained from P-S suspension log test (red line). Cyan shaded region indicates ($T_{Site,Vs}$)/4 of the randomized Vs profiles (transition period).

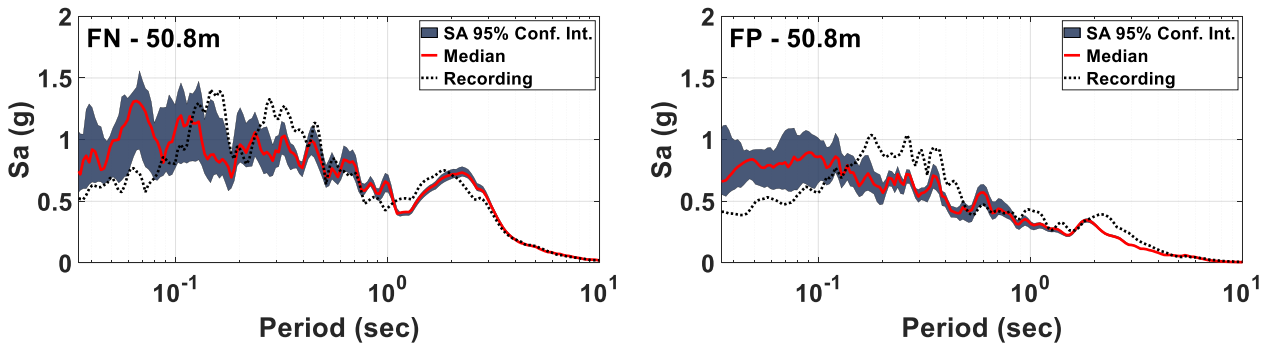

Fig. 4. 2D FN and FP response spectra for the depth of 50.8m below the ground surface (the depth of accelerometer 2). The data shown includes: predicted response spectra using all of 100 Vs profiles developed considering standard deviation value (σ_{ln} (Vs)) of 0.25 (blue area), recorded at accelerometer 1 (dotted black line), predicted response spectra of the base model with the reference Vs profile obtained from P-S suspension log test (red line).

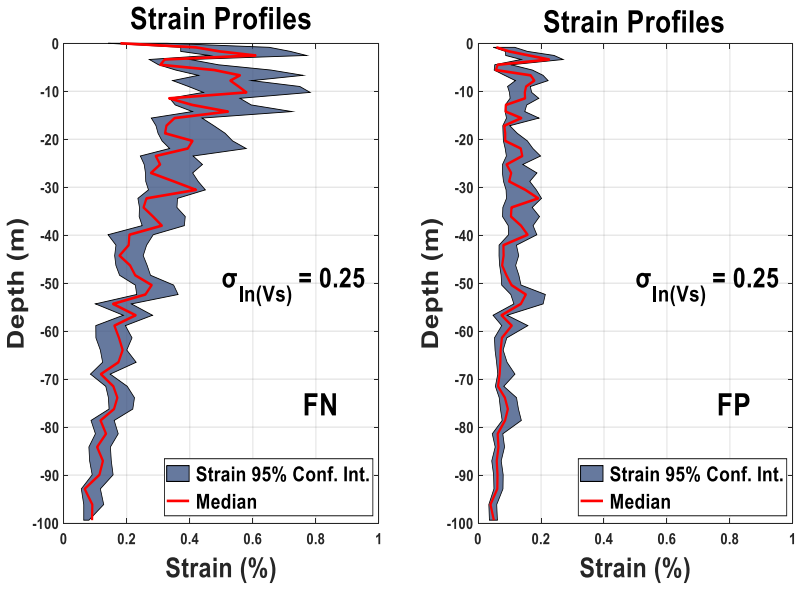

Fig. 5. Peak strain profiles in both FN and FP directions, for the base model as well as the randomized Vs profiles considering a standard deviation value of σ_{ln} (Vs) = 0.25.

The results presented thus far have focused on the realizations for σ_{ln} (Vs) = 0.25; however, as stated in the previous section, the level of uncertainty based on investigations by Toro (1995) may be on the order of σ_{ln} (Vs) = 0.31 to 0.37. Therefore, Fig. 6 and Fig. 7 present the range of variability in response spectra for σ_{ln} (Vs) = 0.15, 0.25, and 0.35 for the FN and FP response spectra for the depths of 2.4m and 50.8m below the ground surface, respectively. As one might expect, the variability of the site response increases substantially when the variability of the Vs profile increases.

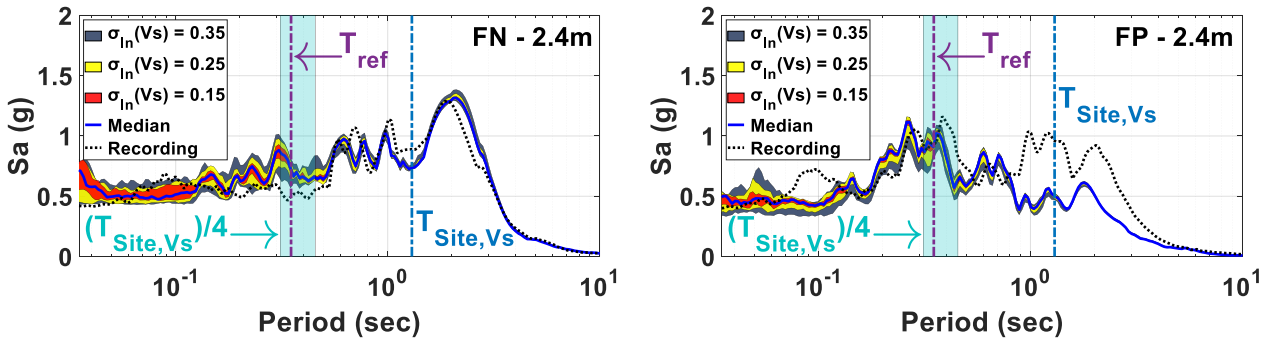

Fig. 6. 2D FN and FP response spectra for the depth of 2.4m below the ground surface (the depth of accelerometer 1). The data shown includes: predicted response spectra using all of 100 Vs profiles developed considering standard deviation value (σ_{ln} (Vs)) of 0.35 (blue area), 0.25 (yellow area), 0.15 (red area), recorded at accelerometer 1 (dotted black line), predicted response spectra of the base model with the reference Vs profile obtained from P-S suspension log test (blue line). Cyan shaded region indicates $(T_{Site,Vs})/4$ of the randomized Vs profiles (transition period).

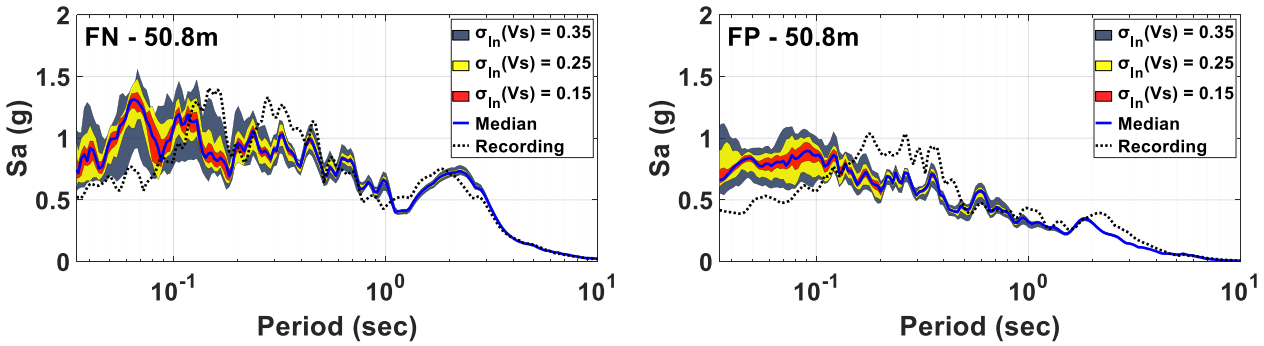

Fig. 7. 2D FN and FP response spectra for the depth of 50.8m below the ground surface (the depth of accelerometer 2). The data shown includes: predicted response spectra using all of 100 Vs profiles developed considering standard deviation value (σ_{ln} (Vs)) of 0.35 (blue area), 0.25 (yellow area), 0.15 (red area), recorded at accelerometer 1 (dotted black line), predicted response spectra of the base model with the reference Vs profile obtained from P-S suspension log test (blue line).

4. Conclusions

In this study, the effects of uncertainties associated with the small-strain Vs profiles on nonlinear site response analysis results have been assessed, considering the Service Hall Array (SHA) near the Kashiwazaki-Kariwa Nuclear Power Plant (KKNPP) in Japan. The Latin Hypercube Sampling (LHS) technique was used to generate Vs profiles (100 realizations) for three different levels of uncertainty that were selected to be representative for the site based on available codes and reports. Results in terms of response spectra at the ground surface and in the middle of the downhole array have been compared with the recordings and predicted response of the base model, with the reference Vs profile obtained from P-S suspension log test, and the biases attributed to Vs profile randomization, as well as the total biases within the system have been presented.

The results show that the standard deviation of the responses, for both FN and FP directions, is much greater at short periods than long periods. The transition period has been defined based on the predominant site period, and the variability of the response decrease considerably for periods longer than $(T_{site,Vs})/4$ of the randomized Vs profiles (transition period). It was expected that the small-strain Vs profile would mainly affect the results for periods shorter than the transition period and this expectation has been generally confirmed through observation of a relatively small standard deviation in the responses for longer periods. Some variability extending to periods greater than the transition period is mainly attributed to nonlinearity of the soil which is amplified by variations in the backbone curves to comply with the specified shear strength.

The results suggest that the standard deviation of the responses is partly a function of the strain level within the soil layers (for example: significant variability of the responses extends to greater periods in the FN direction than the FP direction due to higher shaking intensity). The results also demonstrate that by increasing the standard deviation values for sampling σ_{ln} (Vs), the standard deviation of the responses increases.

5. Acknowledgements

We would like to acknowledge that the ground motion data used in this study belongs Tokyo Electric Power Company, and the distribution license of the data belongs to Japan Association for Earthquake Engineering. The first author also would like to thank Dr. Istrati for his support with LS-Dyna.

6. References

[1] Motamed, R., Stanton, K., Almufti, I., Ellison, K., & Willford, M. (2016). Improved approach for modeling nonlinear site response of highly strained soils: case study of the service hall array in Japan. Earthquake Spectra, 32(2), 1055-1074.

[2] Li, G., Motamed, R., & Dickenson, S. (2018). Evaluation of one-dimensional multi-directional site response analyses using geotechnical downhole array data in California and Japan. *Earthquake Spectra*, *34*(1), 349-376.

[3] Yee, E., Stewart, J. P., & Tokimatsu, K. (2013). Elastic and large-strain nonlinear seismic site response from analysis of vertical array recordings. *Journal of Geotechnical and Geoenvironmental Engineering*, *139*(10), 1789-1801.

[4] Stewart, J. P., & Kwok, A. O. (2008). Nonlinear seismic ground response analysis: Code usage protocols and verification against vertical array data. In Geotechnical earthquake engineering and soil dynamics IV (pp. 1-24).

[5] Passeri, F., Foti, S., Cox, B. R., & Rodriguez-Marek, A. (2019). Influence of epistemic uncertainty in shear wave velocity on seismic ground response analyses. *Earthquake Spectra*, *35*(2), 929-954.

[6] Teague, D. P., Cox, B. R., & Rathje, E. M. (2018). Measured vs. predicted site response at the Garner Valley Downhole Array considering shear wave velocity uncertainty from borehole and surface wave methods. *Soil Dynamics and Earthquake Engineering*, *113*, 339-355.

[7] Park, H. C., Nah, B. C., & Lim, H. D. (2016). Shear wave velocity profile considering uncertainty caused by spatial variation of material property in core zone of fill dam. Journal of the Korean Geotechnical Society, 32(11), 51-60.

[8] Griffiths, S. C., Cox, B. R., Rathje, E. M., & Teague, D. P. (2016). Surface-wave dispersion approach for evaluating statistical models that account for shear-wave velocity uncertainty. Journal of Geotechnical and Geoenvironmental Engineering, 142(11), 04016061.

[9] Passeri, F. (2019). *Development of an advanced geostatistical model for shear wave velocity profiles to manage uncertainties and variabilities in Ground Response Analyses* (Doctoral dissertation, Ph. D. dissertation, Politecnico di Torino).

[10] Bahrampouri, M., Rodriguez-Marek, A., & Bommer, J. J. (2019). Mapping the uncertainty in modulus reduction and damping curves onto the uncertainty of site amplification functions. *Soil Dynamics and Earthquake Engineering*, *126*, 105091.

[11] Tran, T. T., Han, S. R., & Kim, D. (2018). Effect of probabilistic variation in soil properties and profile of site response. Soils and Foundations, 58(6), 1339-1349.

[12] Darendeli, M. B. (2001). Development of a new family of normalized modulus reduction and material damping curves.

[13] Pehlivan, M., Rathje, E. M., & Gilbert, R. B. (2016). Factors influencing soil surface seismic hazard curves. Soil Dynamics and Earthquake Engineering, 83, 180-190.

[14] Rathje, E. M., Kottke, A. R., & Trent, W. L. (2010). Influence of input motion and site property variabilities on seismic site response analysis. Journal of geotechnical and geoenvironmental engineering, 136(4), 607-619.

[15] Baturay, M. B., and Stewart, J. P., 2003. Uncertainty and bias in ground-motion estimates from ground response analyses, Bulletin of the Seismological Society of America 93, 2025–2042.

[16] Kaklamanos, J., Bradley, B. A., Thompson, E. M., & Baise, L. G. (2013). Critical parameters affecting bias and variability in site-response analyses using KiK-net downhole array data. Bulletin of the Seismological Society of America, 103(3), 1733-1749.

[17] Kaklamanos, J., Baise, L. G., Thompson, E. M., & Dorfmann, L. (2015). Comparison of 1D linear, equivalent-linear, and nonlinear site response models at six KiK-net validation sites. Soil Dynamics and Earthquake Engineering, 69, 207-219.

[18] Assimaki, D., & Li, W. (2012). Site-and ground motion-dependent nonlinear effects in seismological model predictions. Soil Dynamics and Earthquake Engineering, 32(1), 143-151.

[19] Assimaki, D., Li, W., Steidl, J., & Schmedes, J. (2008). Quantifying nonlinearity susceptibility via site-response modeling uncertainty at three sites in the Los Angeles Basin. Bulletin of the Seismological Society of America, 98(5), 2364-2390.

[20] Abrahamson, N. A., & Bommer, J. J. (2005). Probability and uncertainty in seismic hazard analysis. Earthquake spectra, 21(2), 603-607.

[21] Mulargia, F., Stark, P. B., & Geller, R. J. (2017). Why is probabilistic seismic hazard analysis (PSHA) still used? Physics of the Earth and Planetary Interiors, 264, 63-75.

[22] Thompson, E. M., Baise, L. G., Tanaka, Y., & Kayen, R. E. (2012). A taxonomy of site response complexity. Soil Dynamics and Earthquake Engineering, 41, 32-43.

[23] Tao, Y., & Rathje, E. (2020). Taxonomy for evaluating the site-specific applicability of one-dimensional ground response analysis. Soil Dynamics and Earthquake Engineering, 128, 105865.

[24] Toro, G. R. (1995). Probabilistic models of site velocity profiles for generic and site-specific ground-motion amplification studies. *Technical Rep*, *779574*.

[25] Kottke, A. R., & Rathje, E. M. (2008). Technical manual for Strata. University of California, Berkeley.

[26] Electric Power Research Institute (EPRI), 2013. Seismic Evaluation Guidance: Screening, Prioritization and Implementation Details (SPID) for the Resolution of Fukushima Near-Term Task Force Recommendation 2.1: Seismic, Report 1025287, Palo Alto, CA.

[27] Moss, R. E. S. (2008). Quantifying measurement uncertainty of thirty-meter shear-wave velocity. Bulletin of the Seismological Society of America, 98(3), 1399-1411.

[28] Teague, D. P., & Cox, B. R. (2016). Site response implications associated with using non-unique vs profiles from surface wave inversion in comparison with other commonly used methods of accounting for vs uncertainty. Soil Dynamics and Earthquake Engineering, 91, 87-103.

[29] Huntington, D. E., & Lyrintzis, C. S. (1998). Improvements to and limitations of Latin hypercube sampling. Probabilistic engineering mechanics, 13(4), 245-253.

[30] Shields, M. D., & Zhang, J. (2016). The generalization of Latin hypercube sampling. Reliability Engineering & System Safety, 148, 96-108.

[31] Tokimatsu, K., & Arai, H. (2008). Dynamic soil behavior and rock outcrop motion back-calculated from downhole array records at kashiwazaki-kariwa nuclear power plant in the 2007 niigata-ken chuetsu-oki earthquakes. In Proc. 5th Int. Conf. on Urban Earthquake Eng (pp. 4-5).

[32] PI, J. P. S., & Yee, E. (2012). Nonlinear site response and seismic compression at vertical array strongly shaken by 2007 Niigata-ken Chuetsu-oki earthquake.

[33] PI, J. P. S., & Yee, E. (2012). Nonlinear site response and seismic compression at vertical array strongly shaken by 2007 Niigata-ken Chuetsu-oki earthquake.

[34] Menq, F. Y. (2003). *Dynamic properties of sandy and gravelly soils* (Doctoral dissertation).

[35] Electric Power Research Institute (EPRI). (2012). Seismic evaluation guidance: Screening, prioritization and implementation details (SPID) for the resolution of Fukushima near-term task force recommendation 2.1: Seismic.

